INCREMENTS IN AEROFOIL LIFT COEFFICIENT AT ZERO ANGLE OF ATTACK AND IN MAXIMUM LIFT COEFFICIENT DUE TO DEPLOYMENT OF A TRAILING-EDGE SPLIT FLAP, WITH OR WITHOUT A LEADING-EDGE HIGH-LIFT DEVICE, AT LOW SPEEDS

1. NOTATION AND UNITS

		SI	*British*
A	parameter in Equation (4.10) for T, Equation (4.11)		
a_t	theoretical rate of change of lift coefficient with trailing-edge flap deflection, Equation (4.4)	rad^{-1}	rad^{-1}
C_{Lm}	maximum lift coefficient of aerofoil with high-lift devices deployed, based on c		
C_{L0}	lift coefficient at zero angle of attack for aerofoil with high-lift devices deployed, based on c		
ΔC_{Lm}	increment in maximum lift coefficient due to deployment of high-lift devices, based on c, Equation (3.2)		
ΔC_{Lml}	increment in maximum lift coefficient due to deployment of leading-edge high-lift device, based on c, see Item No. 94027		
ΔC_{Lmt}	increment in maximum lift coefficient due to deployment of trailing-edge flap, based on c, Equation (3.4)		
$\Delta C'_{Lmt}$	increment in maximum lift coefficient due to deployment of trailing-edge split flap, based on c', Equation (4.9), at datum Reynolds number $R_c = 3.5 \times 10^6$		
$(\Delta C'_{Lmt})_d$	datum value of $\Delta C'_{Lmt}$ for uncambered basic aerofoil with split flap of $c_t/c = 0.2$ at $\delta_t^\circ = 60^\circ$, Figure 2		
ΔC_{L0}	increment in lift coefficient at zero angle of attack due to deployment of high-lift devices, based on c, Equation (3.1)		
ΔC_{L0l}	increment in lift coefficient at zero angle of attack due to deployment of leading-edge high-lift device, based on c, see Item No. 94027		
ΔC_{L0t}	increment in lift coefficient at zero angle of attack due to deployment of trailing-edge flap, based on c, Equation (3.3)		
$\Delta C'_{L0t}$	increment in lift coefficient at zero angle of attack due to deployment of trailing-edge split flap, based on c', Equation (4.5)		
$(\Delta C'_{L0t})_d$	datum value of $\Delta C'_{L0t}$ for basic aerofoil with split flap of $c_t/c = 0.2$ at $\delta_t^\circ = 60^\circ$, Figure 1		

c	basic (plain) aerofoil chord (*i.e.* chord with high-lift devices undeployed), see Sketch 4.1	m	ft
c'	extended aerofoil chord (*i.e.* chord with high-lift devices deployed), see Sketch 4.1	m	ft
c_t	chord of trailing-edge split flap, see Sketch 4.1	m	ft
Δc_l	chord extension due to deployment of leading-edge device, see Sketch 4.1	m	ft
F_R	factor for effect of Reynolds number on ΔC_{Lml} and ΔC_{Lmt}, see Equation (3.5)		
J_{sp}	correlation factor (efficiency factor) for split flap, Equation (4.2)		
K_{tm}	correlation factor for flap deflection, Equation (4.8)		
K_{t0}	correlation factor for flap deflection, Equation (4.3)		
M	free-stream Mach number		
R_c	Reynolds number based on free-stream conditions and aerofoil chord c		
T	theoretical value of $\Delta C'_{Lmt}/\Delta C'_{L0t}$ Equation (4.10) or Figure 3		
t	maximum thickness of aerofoil	m	ft
x	chordwise distance aft from basic aerofoil leading edge	m	ft
x_{lm}	chordwise location of z_{lm}	m	ft
x'_s	chordwise location of boundary-layer separation measured from leading-edge of extended chord	m	ft
z_{cm}	maximum height of camber line of basic aerofoil	m	ft
z_{lm}	maximum lower-surface ordinate of basic aerofoil	m	ft
$z_{u}1.25$	upper-surface ordinate at $x = 0.0125c$ of thickness distribution for basic aerofoil	m	ft
δ_t, δ_t°	deflection of trailing-edge flap, positive trailing edge down, see Sketch 4.1	rad, deg	rad, deg
ρ_l	leading-edge radius of basic aerofoil, see Sketch 4.1	m	ft

Subscripts

$( )_{expt}$ denotes experimental value

$( )_{pred}$ denotes predicted value

2. INTRODUCTION

2.1 Scope of the Item

This Item provides semi-empirical methods for estimating the incremental effects on aerofoil lift at zero angle of attack and on maximum lift due to the deployment of trailing-edge split flaps, with or without the deployment of leading-edge high-lift devices, at low speeds.

Section 3 summarises the equations relating the contributions to the total lift increments at zero angle of attack and at maximum lift arising from the deployment of leading-edge high-lift devices and trailing-edge flaps. The contributions from leading-edge high-lift devices are obtainable from Derivation 6. Section 4 presents methods whereby the contributions from trailing-edge split flaps are obtained.

Section 5 concerns applicability and accuracy, Section 6 gives the Derivation and References and Section 7 presents two detailed examples illustrating the use of the methods.

2.2 Application of Data to Calculation of Total Lift Coefficient Values C_{L0} and C_{Lm}

In order to use the data obtained from the present Item in the wider context in which the total lift coefficient at zero angle of attack, C_{L0}, and at maximum lift, C_{Lm}, are required for an aerofoil with high-lift devices deployed, it is necessary to refer to Item No. 94026 (Reference 8). That Item acts as an introduction to, and a link between, the Items in the complete series dealing with the incremental effects of high-lift device deployment on aerofoil lift at zero angle of attack and on maximum lift. It describes how the incremental effects are summed and added to the contributions from the basic (*i.e.* plain) aerofoil to give the total values C_{L0} and C_{Lm}.

3. LIFT COEFFICIENT INCREMENTS ΔC_{L0} AND ΔC_{Lm}

The increments in the lift coefficient at zero angle of attack, ΔC_{L0}, and at maximum lift, ΔC_{Lm}, due to the deployment of a leading-edge high-lift device and a trailing-edge flap on an aerofoil are given by the sum of the individual increments, *i.e.*

$$\Delta C_{L0} = \Delta C_{L0l} + \Delta C_{L0t} \tag{3.1}$$

and

$$\Delta C_{Lm} = \Delta C_{Lml} + \Delta C_{Lmt}. \tag{3.2}$$

The increments in Equations (3.1) and (3.2) are based on the chord, c, of the basic aerofoil.

The values of ΔC_{L0l} and ΔC_{Lml} for various leading-edge high-lift devices are obtainable from Item No. 94027 (Derivation 6).

For correlation purposes it is more convenient to present the right-hand sides of Equations (3.1) and (3.2) in terms of increments based on the aerofoil extended chord c'. Also, whereas values of ΔC_{L0l} and ΔC_{L0t}

can be taken to be independent of Reynolds number, values of ΔC_{Lml} and ΔC_{Lmt} are influenced by Reynolds number. Thus, for a general trailing-edge flap, Item No. 94028 (Derivation 7) shows that

$$\Delta C_{L0t} = \frac{c'}{c}\Delta C'_{L0t} \tag{3.3}$$

and

$$\Delta C_{Lmt} = F_R \frac{c'}{c}\Delta C'_{Lmt} \tag{3.4}$$

where

$$F_R = 0.153\log_{10}R_c\,. \tag{3.5}$$

The value of $\Delta C'_{Lmt}$ in Equation (3.4) is therefore appropriate to the datum Reynolds number $R_c = 3.5 \times 10^6$, for which $F_R = 1$, (see Section 5).

The values of $\Delta C'_{L0t}$ and $\Delta C'_{Lmt}$ in Equations (3.3) and (3.4) are determined for trailing-edge split flaps by the methods of Section 4.

4. LIFT COEFFICIENT INCREMENTS $\Delta C'_{L0t}$ AND $\Delta C'_{Lmt}$

First approximations to the lift coefficient increments due to the deployment of trailing-edge flaps can be obtained from the theory for an equivalent thin hinged plate with empirical correlation factors to account for the geometry of practical aerofoils and flaps. To make some allowance for the effects of chord extension in the theory the flap chord ratio and the lift coefficient increments are based on the aerofoil extended chord. This approach was used in Derivation 5 and was the basis for the methods developed for plain trailing-edge flaps in Item No. 94028 (Derivation 7), which was used as a model for the methods given in the present Item for trailing-edge split flaps, see Sections 4.1 and 4.2.

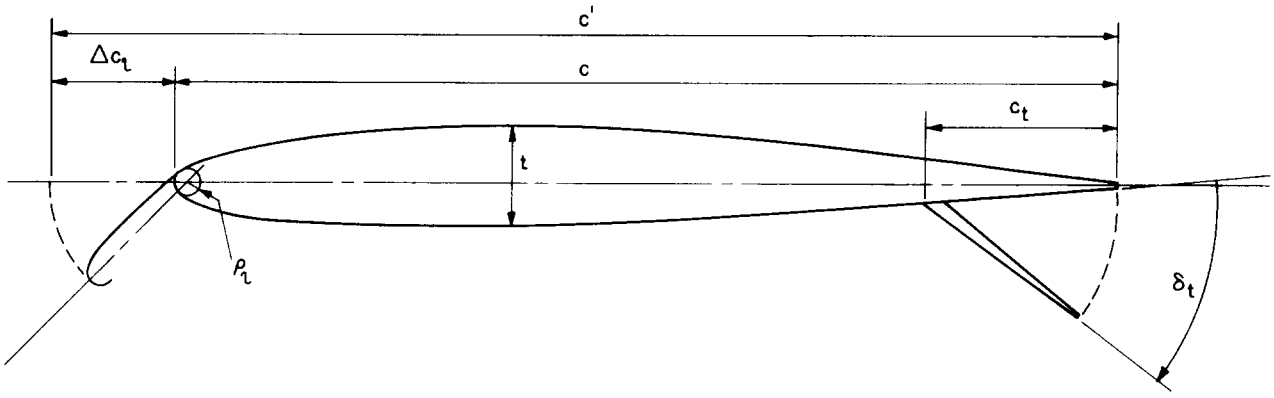

Sketch 4.1 Trailing-edge split flap with typical leading-edge high-lift device (Krüger flap)

4.1 Increment in Lift Coefficient at Zero Angle of Attack

The increment in lift coefficient at zero angle of attack due to the deployment of a trailing-edge split flap is

$$\Delta C'_{L0t} = J_{sp} a_t \delta_t \tag{4.1}$$

where J_{sp} is an empirical correlation (or efficiency) factor, given by

$$J_{sp} = (\Delta C'_{L0t})_d K_{t0} \tag{4.2}$$

where $(\Delta C'_{L0t})_d$ is the datum value for a split flap on the basic aerofoil with $c_t/c = 0.2$ deflected to $\delta_t^\circ = 60^\circ$. The choice of this datum condition was dictated by the preponderance of experimental data available in Derivation 4 for that configuration.

The correlation factor K_{t0} depends only on flap deflection and is given by

$$K_{t0} = 0.41 - 0.13\delta_t = 0.41 - 0.00227\delta_t^\circ. \tag{4.3}$$

The parameter a_t in Equation (4.1) is the theoretical rate of change of lift coefficient with respect to the deflection δ_t, positive trailing edge down, at constant angle of attack, given by thin plate theory in Item No. 94028, whence

$$a_t = 2\left\{\pi - \cos^{-1}(2c_t/c' - 1) + [1 - (2c_t/c' - 1)^2]^{½}\right\}. \tag{4.4}$$

Equation (4.1) can therefore be written, using Equations (4.2) to (4.4), as

$$\boxed{\Delta C'_{L0t} = (0.82 - 0.26\delta_t)\delta_t\left\{\pi - \cos^{-1}(2c_t/c' - 1) + [1 - (2c_t/c' - 1)^2]^{½}\right\}(\Delta C'_{L0t})_d}. \tag{4.5}$$

In Equation (4.5), c_t is the chord of the split flap and c' is the aerofoil extended chord, which from Sketch 4.1 is

$$c' = c + \Delta c_l. \tag{4.6}$$

The value of Δc_l for a variety of leading-edge high-lift devices is obtained from Item No. 94027.

The value of $(\Delta C'_{L0t})_d$ is obtained from Figure 1 and is dependent on $-z_{lm}/c$ for the basic aerofoil and its chordwise location x_{lm}/c, see sketch on Figure 1.

The value of $\Delta C'_{L0t}$ is then used in Equation (3.3) to determine ΔC_{L0t}.

4.2 Increment in Maximum Lift Coefficient

Unlike plain trailing-edge flaps (Item No. 94028) there is no simple relationship between $\Delta C'_{Lmt}$ and $\Delta C'_{L0t}$ for split flaps and the increment in maximum lift coefficient is calculated directly as

$$\Delta C'_{Lmt} = [(\Delta C'_{Lmt})_d - 8(z_{cm}/c)]K_{tm}T\mathrm{a}_t\delta_t \tag{4.7}$$

where $(\Delta C'_{Lmt})_d$ is the datum value for a split flap with $c_t/c = 0.2$ deflected to $\delta_t^\circ = 60^\circ$ on the uncambered basic aerofoil. The datum value is adjusted to allow for camber by means of the empirical term $8(z_{cm}/c)$, where z_{cm} is the maximum height of the camber line.

The correlation factor K_{tm} depends only on flap deflection angle and is given by

$$K_{tm} = 0.95 - 0.34\delta_t = 0.95 - 0.00593\delta_t^\circ . \tag{4.8}$$

The parameter T is the theoretical value of the ratio $\Delta C'_{Lmt}/\Delta C'_{L0t}$ and a_t is given by Equation (4.4).

Equation (4.7) can be rewritten, using Equations (4.4) and (4.8) as

$$\boxed{\Delta C'_{Lmt} = (1.9 - 0.68\delta_t)\delta_t\left\{\pi - \cos^{-1}(2c_t/c' - 1) + [1 - (2c_t/c' - 1)^2]^{\frac{1}{2}}\right\}[(\Delta C'_{Lmt})_d - 8(z_{cm}/c)]T.} \tag{4.9}$$

In Equation (4.9) the value of $(\Delta C'_{Lmt})_d$ is obtained from Figure 2 and is dependent on $z_{u1.25}/c$, the dimensionless upper-surface ordinate of the thickness distribution of the basic aerofoil at $x = 0.0125c$, *i.e.* for the basic aerofoil without camber.

The value of T in Equation (4.9) is given in Item No. 94028 as a function of c_t/c' and x'_s/c', the dimensionless location of boundary-layer separation. For an aerofoil with a smooth leading edge and a deployed split flap a value of $x'_s/c' = 0$ is assumed. It is suggested in Item No. 94028 that the parameter T could be used as a means of accounting for the effect on $(\Delta C'_{Lmt})$ of the interference between a leading-edge device and a trailing-edge flap, via the choice of x'_s/c'. The magnitude of the interference appears to depend on the trailing-edge flap type, but is generally small. The limited data (Derivation 3) shows that $x'_s/c' = 0$ gives the best correlation for split flaps. For this condition T is given as

$$T = \frac{A}{1 + A} \tag{4.10}$$

where

$$A = \frac{2[(c_t/c')(1 - c_t/c')]^{\frac{1}{2}}}{\pi - \cos^{-1}(2c_t/c' - 1)} . \tag{4.11}$$

Note that $T \to \frac{1}{2}$ as $c_t/c' \to 0$. The variation of T with c_t/c' is given in Figure 3 and the value of c' is given by Equation (4.6).

Finally, with the value of $\Delta C'_{Lmt}$ obtained from Equation (4.9), $\Delta C'_{Lmt}$ is evaluated from Equation (3.4) with F_R given by Equation (3.5).

5. APPLICABILITY AND ACCURACY

5.1 Applicability

Methods are given in this Item for estimating the increments in aerofoil lift coefficient at zero angle of attack and in maximum lift coefficient due to the deployment of a trailing-edge split flap with or without the deployment of a leading-edge high-lift device.

Table 5.1 summarises the parameter ranges covered by the measured data, obtained from Derivations 1 to 4, from which the various correlation parameters have been obtained. Although test data (Derivation 3) were available for trailing-edge split flaps in combination with only one type of leading-edge high-lift device (plain leading-edge flap) it is anticipated that the methods will apply to any of the types of leading-edge device treated in Item No. 94027.

The empirical datum values $(\Delta C'_{L0t})_d$ and $(\Delta C'_{Lmt})_d$ and the camber correction in Equation (4.7) were determined through analysis of the numerous test data in Derivation 4. The correlating parameters K_{t0} (Equation (4.3)) and K_{tm} (Equation (4.8)) were obtained using test data from Derivation 1. Note that the methods were developed from available experimental data, involving "traditional" NACA sections, and so the validation has been limited to the (non-reflex) camber lines associated with those sections.

The value $R_c = 3.5 \times 10^6$ was used as the datum from which to develop the factor F_R applicable to the increment in maximum lift coefficient, see Section 3. Most of the data were at or around this value. The effect of Reynolds number on (ΔC_{L0t}) over the ranges given in Table 5.1 and for higher Reynolds numbers can be assumed to be negligible.

The method of the Item takes no account of Mach number in the increments in maximum lift coefficient due to the deployment of high-lift devices. This is not because such effects are felt to be insignificant, since even at quite low free-stream Mach numbers the local flow around a leading-edge device can attain supersonic velocities. Rather, it is due to the lack of data for Mach numbers greater than 0.17 for the type of high-lift device considered. The use of the Item is therefore restricted to $M \leq 0.2$.

TABLE 5.1 Parameter ranges for test data for trailing-edge split flaps used in the methods of Section 4

Parameter	*Range*
t/c	0.06 to 0.30
ρ_l/c	0.004 to 0.099
$z_{u1.25}/c$	0.006 to 0.074
z_{cm}/c	0 to 0.04
x_{lm}/c	0.12 to 0.50
z_{lm}/c	–0.019 to –0.135
c_t/c	0.1 to 0.4
δ_t°	0 to 105°
$R_c \times 10^{-6}$	2.0 to 6.0
M	0.11 to 0.17

5.2 Accuracy

Sketch 5.1 shows the comparison between predicted and experimental values of ΔC_{L0} due to the deployment of trailing-edge split flaps. Also shown are comparisons for a trailing-edge split flap in combination with a plain leading-edge flap. With few exceptions the predicted and test data for ΔC_{L0} are correlated to within ±10 %.

Similarly Sketch 5.2 presents the corresponding values of the increment in maximum lift coefficient. With few exceptions the data for ΔC_{Lm} are correlated to within ±15 %.

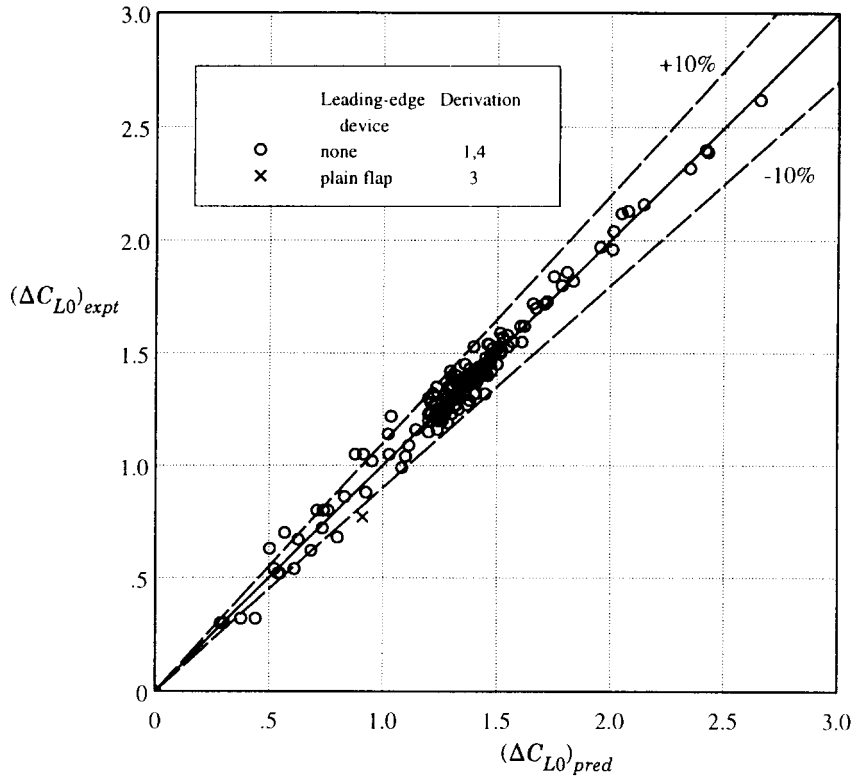

Sketch 5.1 Comparison of predicted and experimental values of ΔC_{L0}

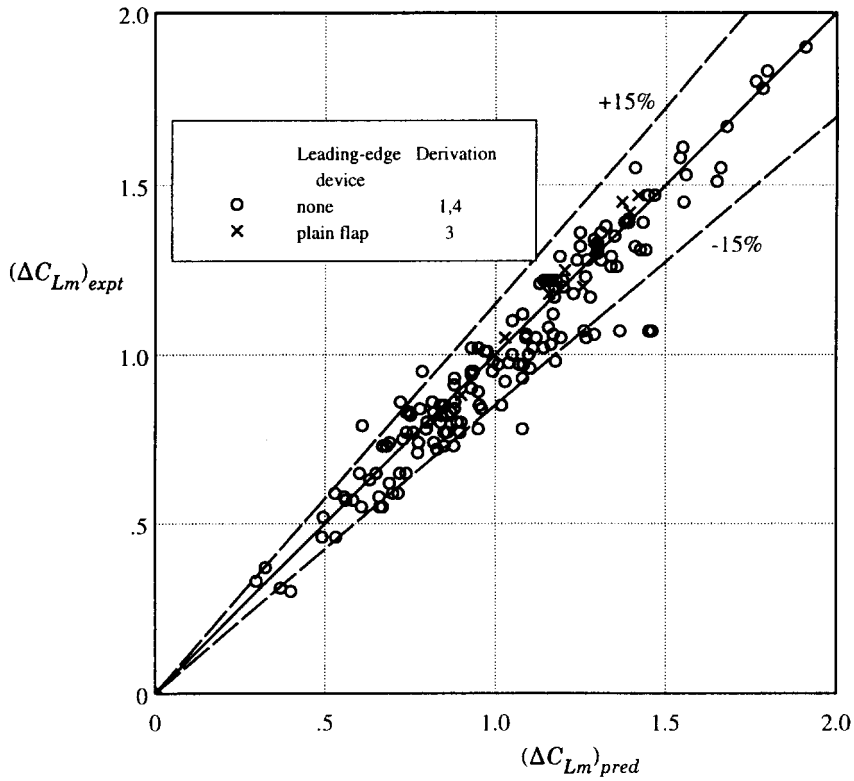

Sketch 5.2 Comparison of predicted and experimental values of ΔC_{Lm}

6. DERIVATION AND REFERENCE

6.1 Derivation

The Derivation lists selected sources of information that have assisted in the preparation of this Item.

1. WENZINGER, C.J. HARRIS, T.A — Wind-tunnel investigation of NACA 23012, 23021 and 23030 airfoils with various sizes of split flap. NACA Rep. 668, 1939.

2. CAHILL, J.F. RACISZ, S.F — Wind-tunnel investigation of seven thin NACA airfoil sections to determine optimum double-slotted-flap configurations*. NACA tech. Note 1545, 1947.

3. KELLY, J.A HAYTER, N.-L.F — Lift and pitching moment at low speeds of the NACA 64A010 airfoil section equipped with various combinations of a leading-edge slat, leading-edge flap, split flap and double-slotted flap. NACA tech. Note 3007, 1953.

4. ABBOTT, I.H. VON DOENHOFF, A.E. — *Theory of Wing Sections*. Dover Publications, New York, 1959.

5. SCHEMENSKY, R.T. — Development of an empirically based computer program to predict the aerodynamic characteristics of aircraft. Volume 1: Empirical methods. Convair Aerospace Division, General Dynamics Corporation. AFFDL TR-73-144 (AD 780 100), 1973.

6. ESDU — Increments in aerofoil lift coefficient at zero angle of attack and in maximum lift coefficient due to deployment of various leading-edge high-lift devices at low speeds. ESDU International, Item No. 94027, 1994.

7. ESDU — Increments in aerofoil lift coefficient at zero angle of attack and in maximum lift coefficient due to deployment of a plain trailing-edge flap, with or without a leading-edge high-lift device, at low speeds. ESDU International, Item No. 94028, 1994.

* This report also contains data for a split flap.

6.2 Reference

The Reference contains information supplementary to that given in this Item.

8. ESDU — Introduction to the estimation of the lift coefficients at zero angle of attack and at maximum lift for aerofoils with high-lift devices at low speeds. ESDU International, Item No. 94026, 1994.

7. EXAMPLES

7.1 Example 1: Trailing-edge Split Flap

The incremental effects on the lift coefficient at zero angle of attack and on the maximum lift coefficient are to be estimated for the deployment of the split flap installed on a smooth NACA 65_2–015 aerofoil as shown in Sketch 7.1. The relevant geometrical data are

Aerofoil	Flap
$c = 4.5\text{ft}$	$c_t = 0.9\text{ft}$
$z_{cm}/c = 0$	$\delta_t^\circ = 60^\circ (\delta_t = 1.047\text{rad.})$
$x_{lm}/c = 0.4$	
$z_{lm}/c = -0.075$	
$z_{u1.25}/c = 0.17$	

The flow conditions are

$M = 0.1$ and $R_c = 4.5 \times 10^6$.

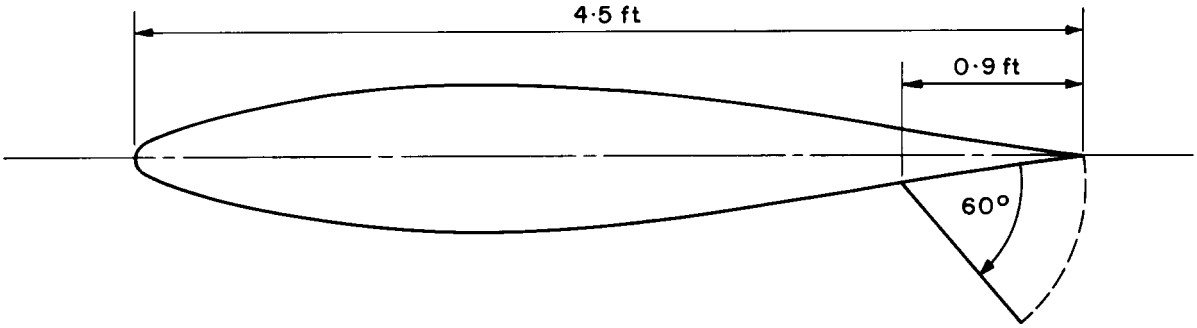

Sketch 7.1

Since the aerofoil is fitted with a split flap the extended chord is that of the basic aerofoil, *i.e.*

$$c' = c = 4.5 \text{ ft},$$

and

$$c_t/c' = 0.9/4.5 = 0.2.$$

Calculation of ΔC_{L0t}:

Figure 1, with $x_{lm}/c = 0.4$ and $z_{lm}/c = -0.075$, gives

$$(\Delta C'_{L0t})_d = 1.42.$$

Therefore, Equation (4.5) gives $\Delta C'_{L0t}$ as

$$\Delta C'_{L0t} = (0.82 - 0.26\delta_t)\delta_t \left\{ \pi - \cos^{-1}(2c_t/c' - 1) + [1 - (2c_t/c' - 1)^2]^{\frac{1}{2}} \right\} (\Delta C'_{L0t})_d$$

$$= (0.82 - 0.26 \times 1.047) \times 1.047 \times \left\{ \pi - \cos^{-1}(2 \times 0.2 - 1) + [1 - (2 \times 0.2 - 1)^2]^{\frac{1}{2}} \right\} \times 1.42$$

$$= 1.407 .$$

Equation (3.3) therefore gives

$$\Delta C_{L0t} = \frac{c'}{c} \Delta C'_{L0t}$$

$$= 1 \times 1.407$$

$$= 1.41 .$$

Calculation of ΔC_{Lmt}:

Figure 2, with $z_{u1.25}/c = 0.017$, gives

$$(\Delta C'_{Lmt})_d = 0.92 .$$

Figure 3, (or Equations (4.10) and (4.11)), with $c_t/c' = 0.2$ gives

$$T = 0.463.$$

Therefore, Equation (4.10)(4.9) gives $\Delta C'_{Lmt}$ as

$$\Delta C'_{Lmt} = (1.9 - 0.68\delta_t)\delta_t \left\{ \pi - \cos^{-1}(2c_t/c' - 1) + [1 - (2c_t/c' - 1)^2]^{\frac{1}{2}} \right\} [(\Delta C'_{Lmt})_d - 8(z_{cm}/c)]T$$

$$= (1.9 - 0.68 \times 1.047) \times 1.047 \times \left\{ \pi - \cos^{-1}(2 \times 0.2 - 1) + [1 - (2 \times 0.2 - 1)^2]^{\frac{1}{2}} \right\} \times$$

$$[0.92 - 8 \times 0] \times 0.463$$

$$= 0.915 .$$

Equation (3.5), with $R_c = 4.5 \times 10^6$, gives

$$F_R = 0.153 \log_{10} R_c$$

$$= 0.153 \times \log_{10}(4.5 \times 10^6)$$

$$= 1.018 .$$

Equation (3.4) then gives

$$\begin{aligned}\Delta C_{Lmt} &= F_R \frac{c'}{c} \Delta C'_{Lmt} \\ &= 1.018 \times 1 \times 0.915 \\ &= 0.93 .\end{aligned}$$

7.2 Example 2: Trailing-edge Split Flap with Krüger Flap

Estimate the effects on the lift coefficient at zero angle of attack and on the maximum lift coefficient of the addition of a Krüger flap to the configuration considered in Example 1, as shown in Sketch 7.2. The relevant geometrical data for the Krüger flap (using the notation of Item No. 94027) are

$$\begin{aligned} c'_l &= 0.45 \text{ ft} \\ \delta_l° &= 38° (\delta_l = 0.663 \text{ rad.}) \\ \rho_l/c &= 0.015 \\ H_l &= 0.045 \text{ ft} \\ x_\tau &= 0.054 \text{ ft} \end{aligned}$$

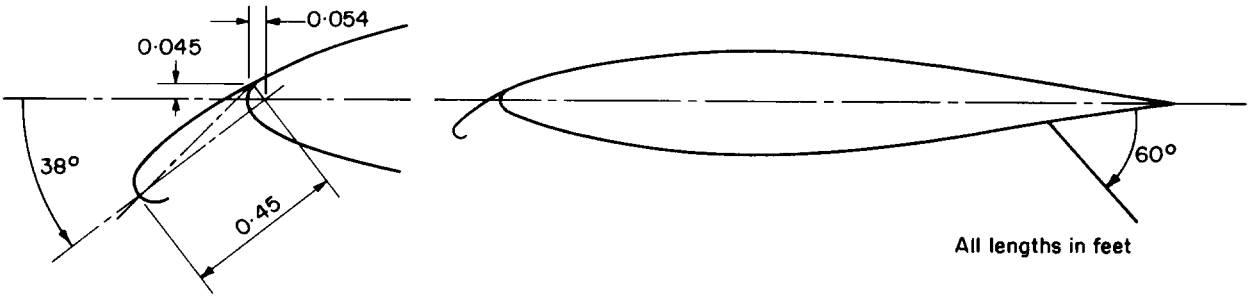

Sketch 7.2

Krüger Flap:

Example 3 of Item No. 94027 details the calculations for ΔC_{Lml} for the Krüger flap used in the present example. Reference to Section 7.3 of Item No. 94027 gives, in the notation of that Item,

$$c' = 4.896 \text{ft}, c_{el}/c' = 0.092, c'/c = 1.088 ,$$

and $\Delta C_{Lml} = 0.707$.

The value of ΔC_{L0l} for the Krüger flap is obtained using the method of Item No. 94027. Table 4.1 of that Item gives

$$K_0 = 1.8 \text{ and } [\Delta C'_{L0l}]_2 = 0 .$$

Equation (3.6) of Item No. 94027 then gives

$$\Delta C'_{L0l} = -2K_0\delta_l\left\{\cos^{-1}(1-2c_{el}/c') - [1-(1-2c_{el}/c')^2]^{\frac{1}{2}}\right\} + [\Delta C'_{L0l}]_2$$

$$= -2\times 1.8\times 0.663\left\{\cos^{-1}(1-2\times 0.092) - [1-(1-2\times 0.092)^2]^{\frac{1}{2}}\right\} + 0$$

$$= -0.091,$$

which with Equation (3.7) of Item No. 94027, gives

$$\Delta C_{L0l} = \frac{c'}{c}\Delta C'_{L0l}$$

$$= 1.088\times(-0.091)$$

$$= -0.099.$$

The values of ΔC_{L0l} and ΔC_{Lml} remain unchanged when the trailing-edge split flap is deployed.

Trailing-edge Split Flap:

ΔC_{L0}:

The differences in the calculation of ΔC_{L0t} relate to the revised value of c' (= 4.896 ft) with the Krüger flap deployed. Therefore, with $(\Delta C'_{L0t})_d = 1.42$ as in Example 1 and $c_t/c' = 0.9/4.896 = 0.184$, Equation (4.5) gives $\Delta C'_{L0t}$ as

$$\Delta C'_{L0t} = (0.82-0.26\delta_t)\delta_t\left\{\pi - \cos^{-1}(2c_t/c'-1) + [1-(2c_t/c'-1)^2]^{\frac{1}{2}}\right\}(\Delta C'_{L0t})_d$$

$$= (0.82-0.26\times 1.047)\times 1.047\times\{\pi - \cos^{-1}(2\times 0.184-1) +$$

$$[1-(2\times 0.184-1)^2]^{\frac{1}{2}}\}\times 1.42$$

$$= 1.353.$$

Equation (3.3) therefore gives

$$\Delta C_{L0t} = \frac{c'}{c}\Delta C'_{L0t}$$

$$= 1.088 \times 1.353$$

$$= 1.472.$$

The total value, ΔC_{L0}, is given by Equation (3.1), *i.e.*

$$\begin{aligned}\Delta C_{L0} &= \Delta C_{L0l} + \Delta C_{L0t} \\ &= -0.099 + 1.472 \\ &= 1.37.\end{aligned}$$

Comparison with Example 1 shows that the Krüger flap deployment reduces the value of ΔC_{L0} by 0.04, or about 3%.

ΔC_{Lm}:

The differences in the calculation of ΔC_{Lmt} again relate to the revised value of c' with the Krüger flap deployed.

Figure 3, (or Equations (4.10) and (4.11)), with $c_t/c' = 0.184$ gives

$$T = 0.466.$$

Therefore, with $(\Delta C'_{Lmt})_d = 0.92$ as in Example 1, $\delta_t = 1.047$ rad., $c_t/c' = 0.184$, $z_{cm}/c = 0$ and $T = 0.466$, Equation (4.9)(4.10) gives $\Delta C'_{Lmt}$ as

$$\Delta C'_{Lmt} = (1.9 - 0.68\delta_t)\delta_t \left\{ \pi - \cos^{-1}(2c_t/c' - 1) + [1 - (2c_t/c' - 1)^2]^{\frac{1}{2}} \right\} [(\Delta C'_{Lmt})_d - 8(z_{cm}/c)]T$$

$$= (1.9 - 0.68 \times 1.047) \times 1.047 \times \left\{ \pi - \cos^{-1}(2 \times 0.184 - 1) + [1 - (2 \times 0.184 - 1)^2]^{\frac{1}{2}} \right\} \times [0.92 - 8 \times 0] \times 0.466$$

$$= 0.886,$$

which, with $F_R = 1.018$ (from Example 1) and $c'/c = 1.088$ in Equation (3.4), gives

$$\begin{aligned}\Delta C_{Lmt} &= F_R \frac{c'}{c} \Delta C'_{Lmt} \\ &= 1.018 \times 1.088 \times 0.886 \\ &= 0.981.\end{aligned}$$

The total value, ΔC_{Lm}, is given by Equation (3.2), *i.e.*

$$\begin{aligned}\Delta C_{Lm} &= \Delta C_{Lml} + \Delta C_{Lmt} \\ &= 0.707 + 0.981 \\ &= 1.69.\end{aligned}$$

Comparison with Example 1 shows that the Krüger flap deployment increases the value of ΔC_{Lm} by 0.76, or about 82%.

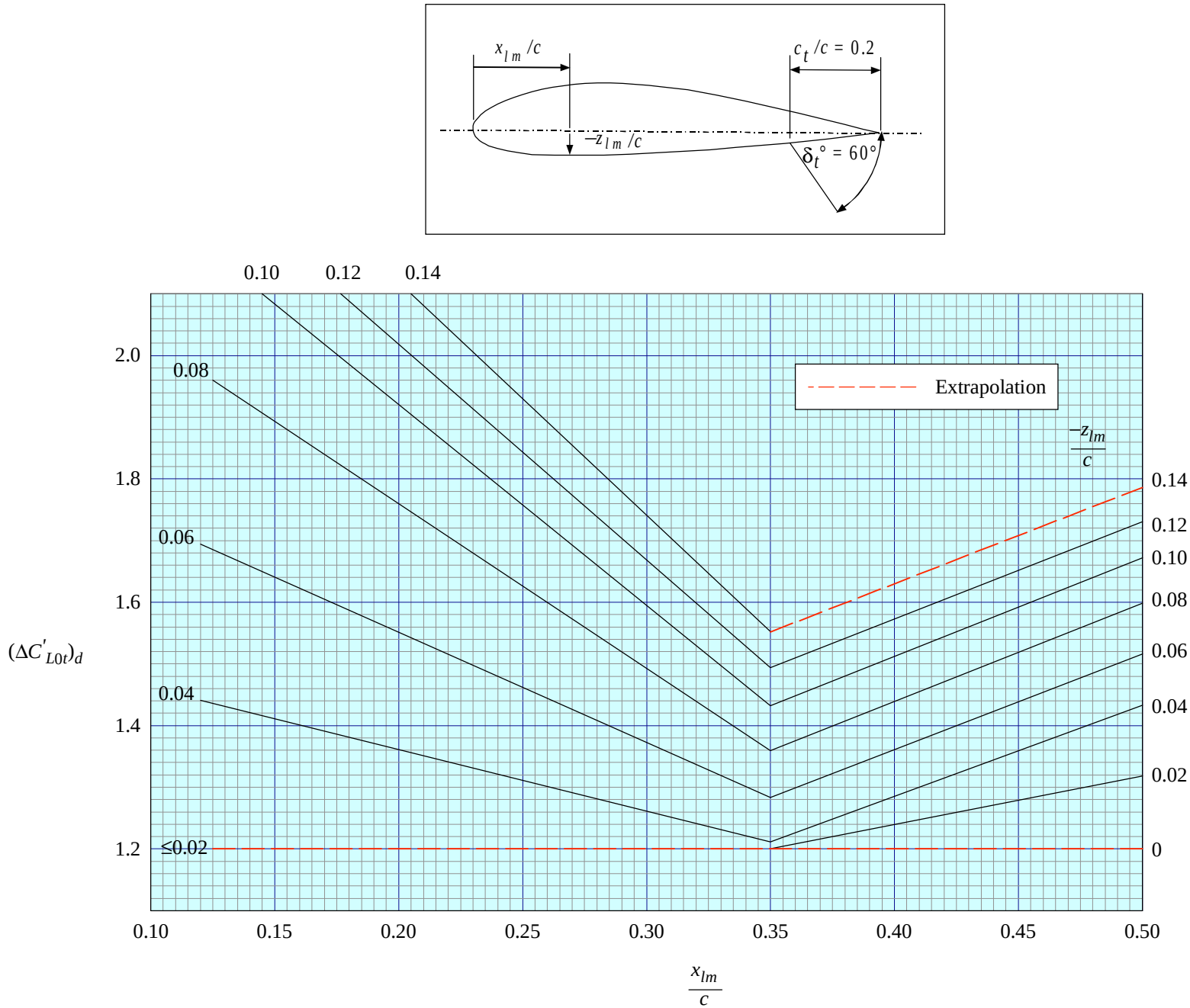

FIGURE 1 DATUM VALUE $(\Delta C'_{L0t})_d$: BASIC AEROFOIL WITH $c_t/c = 0.2$ AND $\delta_t° = 60°$

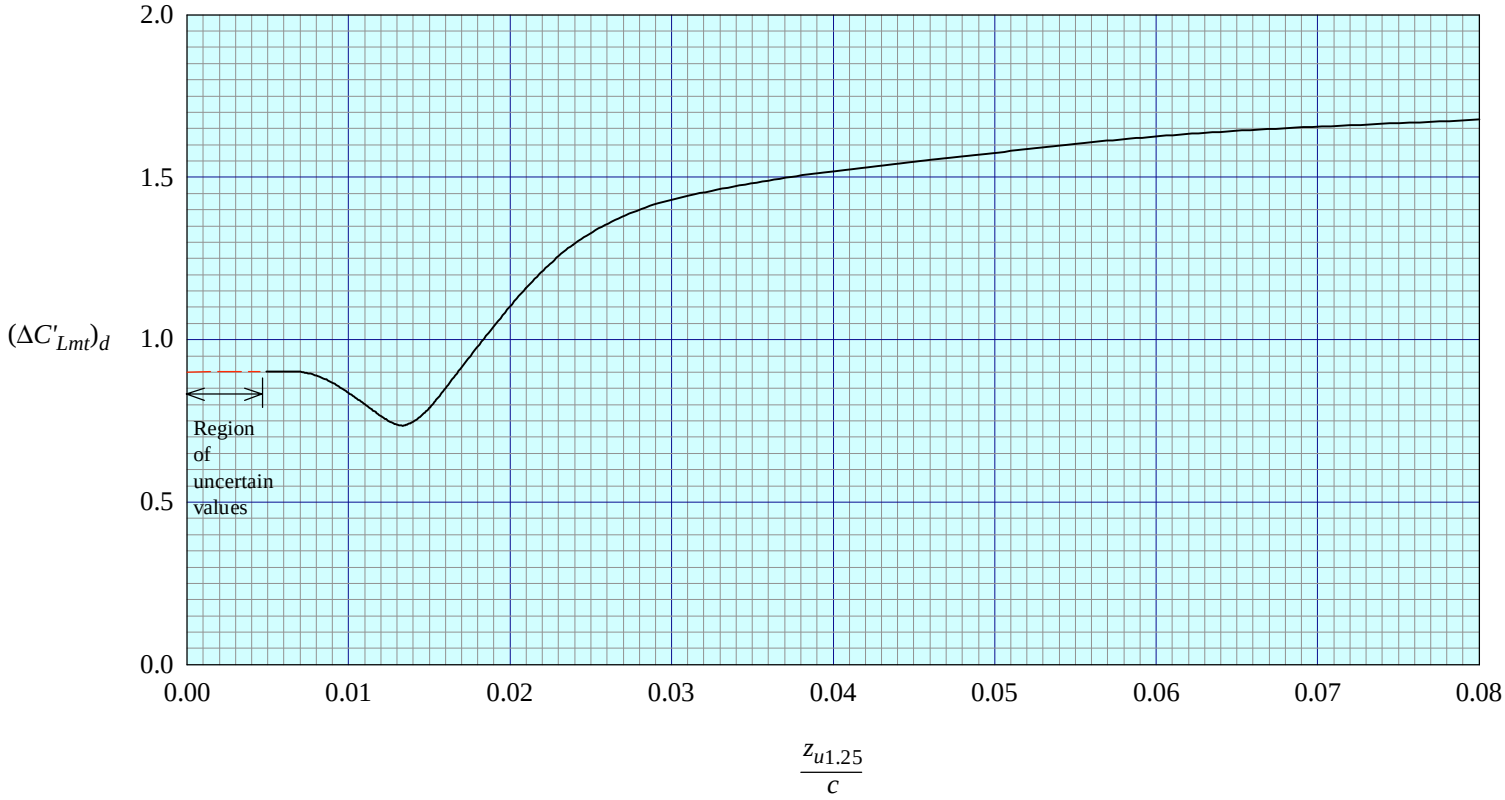

FIGURE 2 DATUM VALUE $(\Delta C'_{Lmt})_d$: UNCAMBERED BASIC AEROFOIL WITH c_t/c = 0.2 AND $\delta_t°$ = 60°

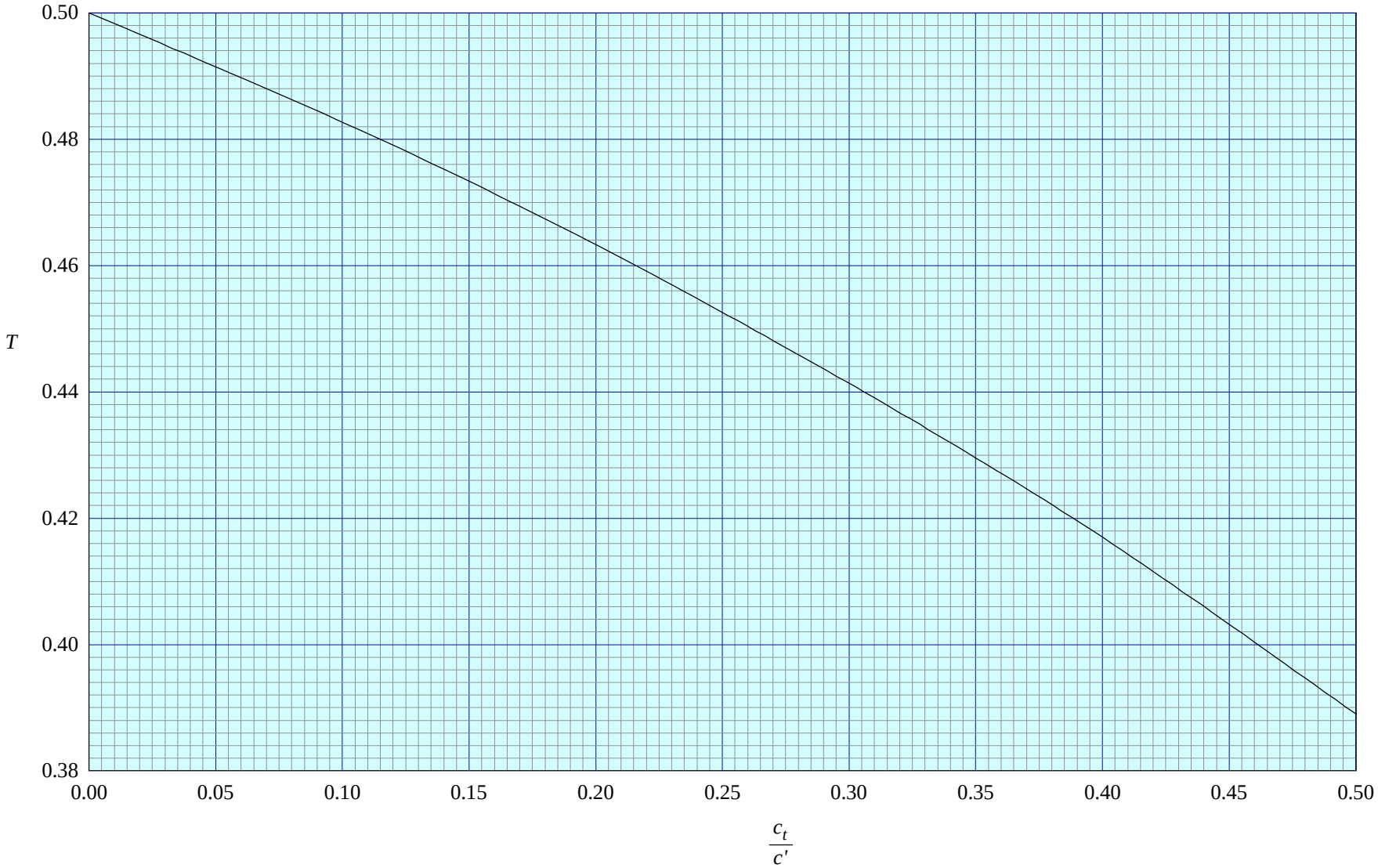

FIGURE 3 THEORETICAL PARAMETER *T*

THE PREPARATION OF THIS DATA ITEM

The work on this particular Item, which supersedes, in part, Item No. 85033, was monitored and guided by the Aerodynamics Committee which first met in 1942 and now has the following membership:

Chairman

Mr H.C. Garner	–	Independent

Members

Mr G.E. Bean*	–	Boeing Commercial Airplane Company, Seattle, Wash., USA
Dr N.T. Birch	–	Rolls-Royce plc, Derby
Mr D. Choo*	–	Northrop Corporation, Pico Rivera, Calif., USA
Dr P.C. Dexter	–	British Aerospace plc, Sowerby Research Centre, Bristol
Mr J.R.J. Dovey	–	Independent
Dr K.P. Garry	–	Cranfield University
Dr H.P. Horton	–	Queen Mary and Westfield College, University of London
Mr P.K. Jones	–	Independent
Mr R. Jordan	–	Independent
Mr K. Karling*	–	Saab-Scania, Linköping, Sweden
Mr M. Maurel	–	Aérospatiale, Toulouse, France
Mr J.B. Newton	–	British Aerospace Defence Ltd, Warton
Mr R. Sanderson	–	Deutsche Aerospace Airbus, Bremen, Germany
Mr A.E. Sewell*	–	McDonnell Douglas, Long Beach, Calif., USA
Mr M.R. Smith	–	British Aerospace Airbus Ltd, Bristol.

* Corresponding Member

The technical work in the assessment of the available information and the construction and subsequent development of the Data Item was carried out under contract by Mr J.R.J. Dovey.